molecular pharmaceutics

Article

pubs.acs.org/molecularpharmaceutics

# *In Silico* Modeling for the Nonlinear Absorption Kinetics of UK-343,664: A P-gp and CYP3A4 Substrate

Bilal S. Abuasal,[†] Michael B. Bolger,[‡] Don K. Walker,[§] and Amal Kaddoumi[†,*]

[†]Department of Basic Pharmaceutical Science, College of Pharmacy, University of Louisiana at Monroe, Monroe, Louisiana 71201, United States

[‡]Simulations Plus, Inc., 42505 10th Street West, Lancaster, California 93534, United States

[§]Department of Drug Metabolism, Pfizer Global Research and Development, Sandwich CT13 9NJ, U.K.

**ABSTRACT:** The aim of this work was to extrapolate *in vitro* and preclinical animal data to simulate the pharmacokinetic parameters of UK-343,664, a P-glycoprotein (P-gp) and CYP3A4 substrate, in human. In addition, we aimed to develop a simulation model to demonstrate the involvement and the controversial complex interaction of intestinal P-gp and CYP3A4 in its nonlinear absorption, first-pass extraction, and pharmacokinetics using the advanced compartmental absorption and transit (ACAT) model. Finally, we aimed to compare the results predicted from the model to the reported findings in human clinical studies. *In situ* perfusion, allometric scaling, PBPK Rodger mechanistic approach, *in vitro* metabolism, and fitting to *in vivo* data were used to mechanistically explain the absorption, distribution and metabolism, respectively. GastroPlus was used to build the integrated simulation model in human for UK-343,664 to mechanistically explain the observed clinical data at 30, 100, 200, 400, and 800 mg oral doses. The measured *in vitro* value for CYP3A4 $K_m$ (465 $\mu$M) in rCYPs was converted to units of $\mu$g/mL, corrected for assumed microsomal binding (17.8%) and applied to all metabolic processes. The measured *in vitro* values of $V_{max}$ for CYP3A4 (38.9 pmol/min/pmol), 2C8, 2C9, 2C19, and 2D6 were used along with the *in vitro* CYP3A4 $K_m$ to simulate liver first pass extraction and systemic clearance. The measured *in vitro* values of $V_{max}$ for CYP3A4 and 2D6 were used along with the *in vitro* CYP3A4 $K_m$ to simulate gut first pass extraction. $V_{max}$ and $K_m$ values for P-gp were obtained by fitting to *in vivo* data and used to simulate gut efflux transport activity. Investigation of the interaction mechanism of P-gp and CYP3A4 in the intestine was achieved by comparing the influence of a virtual knockout of P-gp or gut metabolism on the fraction absorbed, fraction reaching the portal vein, and fraction metabolized in the gut. Comparison between simulation and *in vivo* results showed that the *in silico* simulation provided a mechanistic explanation of the observed nonlinear absorption kinetics of UK-343,664 in human following its administration in the range of 30−800 mg as oral solutions. The simulation results of the pharmacokinetic parameters, AUC and $C_{max}$, by GastroPlus were comparable with those observed *in vivo*. This simulation model is one possible mechanistic explanation of the observed *in vivo* data and suggests that the nonlinear dose dependence could be attributed to saturation of both the efflux transport by P-gp and the intestinal metabolism. However, the concentration ranges for either protein saturation did not overlap and resulted in much greater than dose proportional increases in AUC. At low doses, producing intraenterocyte concentrations below the fitted value of $K_m$ for P-gp, the influence of P-gp appears to be protective and results in a lower fraction of gut 3A4 metabolism. At higher doses, as P-gp becomes saturated the fraction of gut 3A4 extraction increases, and eventually at the highest doses, where 3A4 becomes saturated, the fraction of gut 3A4 extraction again decreases. Such a complex interpretation of this *in vitro*−*in vivo* extrapolation (IVIVE) is another example of the value and insight obtained by physiologically based absorption simulation.

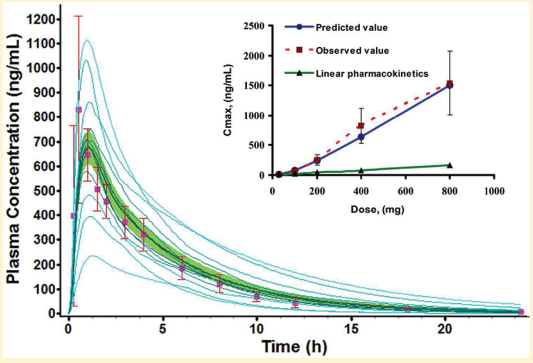


**KEYWORDS:** *in silico modeling, nonlinear pharmacokinetics, intestinal metabolism, P-glycoprotein, GastroPlus*

## INTRODUCTION

The prediction of oral drug absorption continues to be challenging due to the interaction of several factors that determine the absorption process.[1−6] For example, prior to absorption across the mucosal surfaces of the cells lining the gastrointestinal tract (GIT), the drug must be solublized within the fluid of the GIT.[7−10] Once dissolved, the drug will be absorbed into the enterocytes. There are several mechanisms of absorption including passive transcellular diffusion, carrier-mediated transport, paracellular transport, and endocytosis. The absorption and solublization of a drug compound are dependent on numerous physicochemical properties such as size, charge, intrinsic lipophilicity and salt form.[11−14] In general, passive diffusion is the main mechanism for absorption of many lipophilic compounds while the carrier-mediated influx and

**Received:** May 29, 2011
**Revised:** September 24, 2011
**Accepted:** January 20, 2012
**Published:** January 20, 2012

efflux processes determine the absorption of transporter substrates.[15−19] The major collective sites of drug absorption are the intestinal segments which include the duodenum, the jejunum and the ileum.[2,18,20−22] Following the drug entry into enterocyte or hepatocyte cells it is possible for the drug to undergo metabolism, thus limiting its systemic bioavailability. The intestinal tract contains several metabolizing enzymes including CYP3A isoforms.[20,23] CYP3A enzymes represent the principal drug-metabolizing system in the small intestine, are involved in the metabolic clearance of approximately 50% of drugs currently in the market, and account for approximately 80% of the total cytochrome P450 content in the small intestine.[24] Although the total amount of CYP3A expressed in the human small intestine represents approximately 1% of the hepatic estimated amount, considerable drug extraction occurs following absorption of orally administered drugs.[23,25] This is due to the relatively high enterocytic drug concentration and the fact that all molecules absorbed via the transcellular route in the enterocyte are exposed to the CYP enzymes whereas blood flow and hepatocyte uptake are required for CYP exposure in the liver. Also, the low level of protein binding in the intestine increases the fraction of drug exposed to metabolizing enzymes.[26]

In addition to CYP3A, specialized transport proteins, such as P-glycoprotein (P-gp), are present in well-defined regions of the intestinal tract. Intestinal P-gp, an ATP-dependent multidrug efflux transporter, has been established as an active secretion system or an absorption barrier by transporting some drugs from inside intestinal cells back into the lumen.[16,17,27,28] Drug transporters (e.g., P-gp) and metabolic enzymes (e.g., CYP3A4) independently may act to reduce the bioavailability. It has also been found that there are almost completely overlapping substrate specificities between P-gp and CYP3A4. These complicated interactions between a P-gp and CYP3A4 substrate are receiving considerable attention in clinical pharmacotherapeutics and *in vitro*−*in vivo* extrapolation (IVIVE) studies. A number of studies have been reported describing available models and assumptions for such complicated P-gp−CYP3A4 interaction in the intestine.[29−32] For example, Benet (2009) suggested that P-gp increases gut metabolism by CYP3A4 of their substrates by decreasing the influx rate into the enterocytes and by increasing the exposure time to CYP3A4 in the enterocytes.[31] On the other hand, Thakker and colleagues (2006) suggested that P-gp decreases the intestinal metabolism of their substrates.[30] The effect of both CYP3A4 and P-gp when acting in concert during intestinal absorption is difficult to predict. Thus, further understanding of the physiology and biochemistry of the interactive nature of intestinal CYP3A4 and P-gp will be important in defining, controlling, and improving oral bioavailability of CYP3A4/P-gp substrates.[33]

Saturation of the gut efflux transporters and metabolizing enzymes plays an important role in the nonlinear pharmacokinetic behavior of drugs.[34] Nonlinear pharmacokinetics represents a challenge to the successful development of a drug candidate, especially when this behavior occurs across the therapeutic dose range. Such behavior complicates drug therapy due to extensive variability in exposure, which may lead to variable efficacy and/or adverse effects.[33] Nonlinearity in human oral pharmacokinetics may be a result of saturation of clearance processes or effects on intestinal absorption.[35,36] Saturation of intestinal P-gp has been implicated in the nonlinear oral absorption of several drugs including talinolol, celiprolol and UK-343,664.[37,38]

The prediction of nonlinear oral pharmacokinetic behavior prior to initiation of clinical studies would substantially reduce the time and research investment involved in design of first in human clinical studies, and would ultimately contribute to the development of safer drugs. Many *in silico* approaches have been proposed to estimate the absorption and first pass extraction of orally administered drugs. These approaches are based on the incorporation of drug permeability and metabolism data, and enterocytic blood flow together with zonal and cellular heterogeneous distribution of metabolic enzyme and efflux/uptake transporters along the length of the intestine.

In recent years, many dynamic and compartmental models have been developed to account for both special and temporal variables. Among these models are ADAM, Grass, GITA and the advanced compartmental absorption and transit (ACAT) model.[39] These models have been integrated in many software packages that are used for the *in silico* prediction of pharmacokinetic properties from preclinical and *in vitro* data including IDEA, SimCYP, PKSim, and GastroPlus softwares.[34,40−46] GastroPlus is an advanced technology computer program that simulates gastrointestinal absorption, distribution, pharmacokinetics, and optionally pharmacodynamic effects for drugs dosed by oral route in humans and animals. The underlying model in GastroPlus is the ACAT. The physiologically based ACAT model consists of nine compartments corresponding to different segments of the digestive tract and is based on the original compartmental absorption and transit model described by Yu and Amidon.[47] Each compartment is further subdivided to describe drug that is unreleased (when modified release formulations are simulated), undissolved, dissolved, and absorbed. Absorbed drug is defined as the drug that has entered into the enterocytes. Movement of drug between each subcompartment is described by a series of differential equations. The rate of drug flow through the sequential intestinal compartments is determined by the transit time of each compartment. The ACAT model is able to simulate efflux and influx transport processes in the GIT, and was the first to publish the simulation of nonlinear intestinal first pass metabolism from preclinical data using a compartmental absorption and transit model.[43] In addition, the ACAT model accounts for factors such as variation in the pH along the GIT, the physicochemical parameters of the compounds which might influence the dissolution and the absorption of the compounds.[48] In a recent study using GastroPlus to simulate the release, dissolution, absorption, and pharmacokinetics of several generic formulations of carbamazepine, Zhang and colleagues highlighted the importance of physiologically based absorption modeling in Quality by Design in drug development.[49] The unique numerical integration of linear and nonlinear processes governing the absorption in GastroPlus makes it excellent software for the prediction and simulation of drugs showing nonlinear pharmacokinetic behavior like UK-343,664.

UK-343,664 is a potent and specific inhibitor of the human cGMP-specific phosphodiesterase type 5 enzyme (PDE5). PDE5 inhibitors have been effectively used in the treatment of male erectile dysfunction.[38] When the compound was progressed to clinical trials, a marked nonproportionality in the pharmacokinetic profile was observed after oral doses.[38] Potential sources of the nonlinear behavior were considered to

be due to a saturable process governing the systemic availability of UK-343,664. In addition to the possible role of drug metabolizing enzymes in this profile, the transport protein P-gp has also been considered as a potential source.[38,50,51] The structure of UK-343,664 is illustrated in Figure 1.

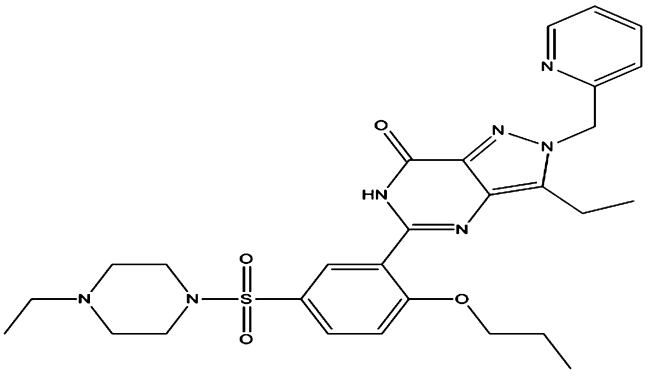

**Figure 1.** Structure of UK-343,664.

The objective of this article is to utilize the preclinical pharmacokinetic data, reported in the literature or obtained in our laboratory, to retrospectively predict and explain the nonlinear pharmacokinetics of UK-343,664, a substrate for P-gp and CYP3A4, and to further investigate the contribution of both proteins in the absorption kinetics of this compound using GastroPlus.

## MATERIAL AND METHODS

To simulate the oral absorption kinetics of dose escalating studies in humans, a number of preclinical tests were used to obtain pharmacokinetics parameters. These tests include data collected from the literature,[38,50,51] or unpublished data provided by Pfizer Global Research and Development (Sandwich, U.K.). In addition, some parameters were obtained experimentally in our laboratory as described below.

**Materials.** UK-343,664 was provided by Pfizer Global Research and Development (Sandwich, U.K.). The chemical structure of this compound is shown in Figure 1. Verapamil hydrochloride was purchased from Sigma-Aldrich (St. Louis, MO). Recombinant CYP3A4 Supersomes and NADPH regenerating systems were purchased from BD Gentest (Woburn, MA). Other chemicals and reagents were obtained from VWR Scientific (West Chester, PA).

**Computer Hardware and Software and Human Clinical Data.** The simulations were performed on a Dell desktop station with Intel core 2 Duo CPU E4400 (2.00 GHz) using GastroPlus version 7.01 software (Simulation Plus Inc., Lancaster, CA). GastroPlus utilizes the ACAT model to predicting the rate and extent of drug absorption from the GIT. It also incorporates intestinal drug efflux and metabolism in its predictions of pharmacokinetic parameters. Human pharmacokinetic profiles of 24 male volunteers given single doses of 30, 100, 200,400 and 800 mg UK-343,664 were provided and published by the department of Drug Metabolism and Clinical Sciences, Pfizer Global Research and Development at Sandwich, U.K..[38]

**Animals.** Male Sprague−Dawley rats weighing 260−400 g were acquired from Harlan Laboratories (Houston, TX). All animal experiments were approved by the Institutional Animal Care and Use Committee of the University of Louisiana at Monroe, and all surgical and treatment procedures were consistent with the IACUC policies and procedures. Rats were maintained at a 12 h light/dark cycle before the study and were fasted 12−14 h with water *ad libitum* prior to each experiment.

***In Situ* Rat Intestinal Perfusion.** *In situ* studies were conducted as reported previously.[50,52] In brief, after an overnight fasting, rats were anesthetized with intramuscular injection of 50 mg/kg ketamine and 10 mg/kg xylazine mixture, followed by intraperitoneal injection of 40 mg/kg pentobarbital. The small intestine was exposed by midline incision, and then approximately 15 cm of upper jejunum (proximal to the duodenum) was externalized. The segments were then flushed with warm normal saline to remove intestinal contents and cannulated with glass cannulas inserted at the inlet and the outlet of each segment and were secured by ligation with silk suture. The inlet tubing of each segment was connected to a 30 mL syringe that was placed in an infusion pump (Harvard apparatus, Holliston, MA). The perfusate was pumped through the lumen at 0.14 mL/min flow rate. The perfusate solution consisted of 5 $\mu$M UK-343,664 in phosphate buffer (pH 6.5) solution containing 500 $\mu$M verapamil. Verapamil was used to inhibit both intestinal P-gp efflux and CYP3A4 metabolism to better predict the passive permeability of UK-343,664 across the intestinal membrane. Following 40 min stabilization to reach steady state, the perfusate was collected in vials at 10 min intervals for 100 min. The samples were analyzed for UK-343,664 concentrations using HPLC.

**Pharmacokinetics of UK-343,664 after Intravenous Administration in Rats.** Rats were anesthetized with 1.2 g/kg urethane dissolved in normal saline by intraperitoneal injection. UK-346,664 (37.5 mg) dissolved in DMSO was intravenously administered via the femoral vein. Blood samples (250 $\mu$L) were taken at 0.04, 0.25, 0.5, 1, 2, 4, 6, 8, and 10 h. Blood samples were centrifuged for 10 min at 10000*g*, and plasma was separated. UK-346,664 was extracted from plasma following precipitation with acetonitrile (1:1, v/v) from which 20 $\mu$L was injected into the HPLC system.

**Solubility Studies of UK-343,664.** The solubility of UK-343,664 was studied at pH 5, 6.8, 7.4, and 8 using the shake flask method.[53] In brief, 0.5 g of the compound was dispersed in 2 mL of phosphate buffer (0.2 M) adjusted to different pH values in amber glass vials. The vials were incubated in a shaker at 37 °C over 48 h to establish equilibrium solubility, and the final pH was measured. After that, samples were centrifuged for 10 min at 5000*g* and the supernatant was then diluted with methanol and injected into the HPLC system to analyze drug concentration in the samples.

**Metabolism Studies Using Recombinant CYP3A4 (Supersomes).** Disappearance of UK-343,664 was characterized in microsomes from baculovirus cells engineered to express CYP3A4 Supersomes. UK-343,664 was incubated in a reaction mixture (1 mL) consisting of NADPH-generating system A (50 $\mu$L) and B (10 $\mu$L) in 100 mM potassium phosphate buffer. Enzyme reactions were initiated by adding 20 pmol of Supersomes in 1 mL total reaction mixture. After incubation at 37 °C in a shaking water bath for 5, 10, 20, 30, 40, and 60 min the reaction was terminated by adding 250 $\mu$L of acetonitrile, and then the reaction mixture was centrifuged at 10000*g* for 10 min and an aliquot of the supernatant was taken and analyzed by HPLC. Data from this kinetic experiment were analyzed by GraphPad Prism (ver 4.01; La Jolla, CA) by an iterative nonlinear least-squares algorithm to obtain $K_m$ and $V_{max}$.

**HPLC Analysis.** Analysis of the UK-343,664 in the metabolism studies, solubility studies, *in situ* perfusion studies, and the rat plasma was carried out using an HPLC method reported by Kaddoumi et al.[50] with some modifications. The method entailed an isocratic Prominence Shimadzu HPLC system (Columbia, MD). The system consisted of SIL 20-AHT auto sampler, SPD-20A UV/vis detector set at wavelength of 230 nm, and LC-20AB pump connected to a Dgu-20A3 degasser. Data acquisition was achieved by Shimadzu LC Solution software version 1.22 SP1. The chromatographic conditions were a Luna 5 $\mu$ C18 column (250 × 4.6 mm i.d.; Phenomenex, Torrance, CA) with mobile phase delivered at 1 mL/min flow rate and consisting of a mixture of phosphate buffer (0.05 M, pH 6.0), acetonitrile and methanol (50:40:10, v/v/v).

**Prediction of UK-343,664 Disposition Parameters.**

*Prediction of the Intestinal Permeability.* Intestinal permeability is a very important parameter to predict the rate of absorption of compounds. There are many models that have been used to predict the permeability such as Caco-2 Transwell permeability model and the PAMPA system.[1,54] However, the *in situ* rat intestinal perfusion model is one of the most reliable models to predict the permeability in human because it is dynamic where most of the transporters and metabolizing enzymes are available, which makes it the best model to predict the intestinal drug interaction with transporters and metabolizing enzymes.[55] Previous *in situ* studies showed that UK-343,664 exhibits nonlinear absorption kinetics with a significant increase in the intestinal permeability ($P_{eff}$) as a function of perfusion concentration of the compound. This pattern of $P_{eff}$ suggested saturation of P-gp and/or CYP3A4 as possible explanations for the nonlinear absorption kinetics.[50]

$P_{eff}$ of UK-343,664 in rats was calculated using the following equation (eq 1):

$$P_{eff} = \frac{-Q \ln\left(\frac{C_t}{C_0}\right)}{2\pi r L} \quad (1)$$

where $Q$ is the perfusate flow rate through the segment (0.14 mL/min), $r$ is the radius of the intestinal lumen (0.2 cm), $L$ is the length of the perfused segment (15 cm), $C_0$ is UK-343,664 concentration at the start of perfusion (from the entry tubing), and $C_t$ is the steady state of UK-343,664 concentration exiting the perfused intestinal segment.

Passive permeability obtained from *in situ* perfusion of UK-343,664 with verapamil in rats was scaled to human $P_{eff}$ using a built-in model in GastroPlus. This model correlates the *in situ* rat permeability values with human $P_{eff}$ values using a regression relationship derived from example compounds where permeability values for such compounds were measured using both techniques for the same compounds.[56] The human $P_{eff}$ value was then integrated with the *in vitro* kinetic parameters of P-gp, $V_{max}$ and $K_m$, to predict the nonlinear behavior.

The built-in ADMET Predictor module in GastroPlus was also used for prediction of human $P_{eff}$ based on the structure properties of the loaded compound. ADMET Predictor has a built-in QSPR (quantitative structure properties relationship) model, which can be used to predict the biopharmaceutical properties of the compound from the structures of the built-in compounds.

*Intestinal P-gp and CYP3A4 Pharmacokinetic Constants.* CYP3A4 is the dominant CYP450 isoform in human enterocytes (~80% of total CYP450). *In vitro* metabolism of UK-343,664 with different recombinant CYPs isoforms showed that CYP3A4 has the greatest ability of the P450s examined to metabolize UK-343,664.[38,51] Based on these facts, the metabolic stability by human CYP3A4 Supersomes was used to predict the *in vitro* $K_m$ and $V_{max}$ values. In our simulations the *in vitro* $V_{max}$ value was scaled to *in vivo* $V_{max}$ using the enzyme amount based scale factors available in GastroPlus.

The *in vitro* $V_{max}$ and $K_m$ values for P-gp were measured using Caco-2 cells and were obtained by Pfizer (unpublished data); the kinetic parameters for CYP3A4 and P-gp were then integrated into the ACAT model. The ACAT model assumes that P-gp and CYP3A4 are present in the same forms with similar intrinsic activity in all parts of the GIT; therefore any change in the rate of flux by P-gp or metabolism by CYP3A4 will be simulated by taking into account the experimentally observed changes in the expression of P-gp and CYP3A4 present in the enterocyte compartments. Although the contribution of CYP2D6 in the metabolism of UK-343,664 was reported to be minimal,[38] CYP2D6 predicted parameters were included in the ACAT physiology along with CYP3A4 parameters to establish maximal simulation of the *in vivo* conditions. In the absence of $K_m$ data for CYPs other than 3A4, it was assumed that all of the included CYP450 isoforms have similar affinity for UK-343,664 and the difference in the reported fraction metabolized after 30 min incubation was attributed to differences in the $V_{max}$. The reported fraction metabolized with Supersomes transfected with CYP3A4 and other CYP450 isoforms was 38, 6, 11, 2, 3 and 3% for CYP3A4, CYP2D6, CYP2C19, CYP2C9 and CYP2C8, respectively.[38] Only intestinal CYP3A4 and CYP2D6 were included in the intestinal compartments because their relative distribution in the small intestine and colon has been reported. We tested the simulation by including CYP2C19 in the gut using the same expression, and distribution as 2D6 and the FDp (fraction reaching portal vein) was decreased by less than 1%.

*Prediction of Volume of Distribution ($V_D$).* There are several methods to predict the $V_D$ including the allometric scaling from preclinical species. In this method, a proportionality is established between $V_D$ at steady state ($V_{Dss}$) and fraction unbound ($fu$) in preclinical species and human, and allometric scaling is used with additional consideration of the interspecies differences in plasma protein binding.[57] Mechanistic models of tissue−plasma concentration ratios are informative and provide a good prediction of the $V_D$. These methods were developed from an understanding of the underlying distribution mechanisms and physiological information. Such methodologies were later refined and investigated by Poulin and Rodgers[58,59] who developed mechanistic equations to predict the affinity of drugs for various tissues and organs, which subsequently permitted $V_{Dss}$ predictions. In our prediction of UK-343,664 $V_{Dss}$, we compared two approaches. In the first approach, as described by Obach and colleagues, we assumed that the $V_D$ of the unbound UK-343,664 and the tissue binding per-weight basis are similar in rats and humans.[57] Solving for the human $V_D$ (L/kg), the following equation was used:

$$V_{D(human)} = \frac{fu_{(human)} V_{D(rat)}}{fu_{(rat)}} \quad (2)$$

where the term $fu$ designates the fraction of drug unbound in the plasma (or serum) of rat or human, and $V_D$(rat) represents $V_D$ at steady state in rat (L/kg).


dx.doi.org/10.1021/mp200275j | Mol. Pharmaceutics 2012, 9, 492−504

Table 1. ACAT Physiological Model Parameters Used in Simulations

| compartment | ASF ($cm^{-1}$) | pH | transit time (h) | volume (mL) | length (cm) | radius (cm) | P-gp expression (rel)[a] | CYP expression (rel)[b] 3A4 | CYP expression (rel)[b] 2D6 |
|---|---|---|---|---|---|---|---|---|---|
| stomach | 0 | 1.3 | 0.1 | 50 | 30 | | 0 | 0 | 0 |
| duodenum | 2.64 | 6 | 0.26 | 48.25 | 15 | 1.6 | 0.539 | $2.09 \times 10^{-3}$ | $2.06 \times 10^{-4}$ |
| jejunum 1 | 2.64 | 6.2 | 0.95 | 175.3 | 62 | 1.5 | 0.645 | $3.26 \times 10^{-3}$ | $4.12 \times 10^{-4}$ |
| jejunum 2 | 2.62 | 6.4 | 0.76 | 139.9 | 62 | 1.34 | 0.723 | $3.26 \times 10^{-3}$ | $4.56 \times 10^{-4}$ |
| ileum 1 | 2.60 | 6.6 | 0.59 | 108.5 | 62 | 1.18 | 0.77 | $1.03 \times 10^{-3}$ | $6.9 \times 10^{-4}$ |
| ileum 2 | 2.59 | 6.9 | 0.43 | 79.48 | 62 | 1.01 | 0.838 | $1.03 \times 10^{-3}$ | $7.19 \times 10^{-4}$ |
| ileum 3 | 2.55 | 7.4 | 0.31 | 56.29 | 62 | 0.85 | 0.908 | $1.03 \times 10^{-3}$ | $4.16 \times 10^{-4}$ |
| cecum | 1.03 | 6.4 | 4.5 | 5.29 | 13.75 | 3.5 | 1 | $3.1 \times 10^{-4}$ | 0 |
| ascending colon | 2.79 | 6.8 | 13.5 | 5.69 | 29 | 2.5 | 1 | $3.1 \times 10^{-4}$ | 0 |

[a]These values were obtained based on the relative distributions as reported by Mouly et al. (2003)[61] and Bruyere et al. (2010).[62] [b]These values were calculated based on the relative distribution to the liver as reported by Paine et al. (1997).[23]

The second approach for predicting $V_D$ was to use Rodgers mechanistic equations for the prediction of tissue-to-plasma water partition coefficients (Kpu). The predicted Kpu values were eventually used to predicting the $V_D$ of UK-343,664. The PBPKPlus module in GastroPlus was used to predict the Kpu values and then used to calculate $V_D$.

*Prediction of Systemic Clearance.* Following intravenous administration of radioactive UK-343,664 to rats and dogs, excretion studies have shown that only 10% of the drug was eliminated as parent compound.[51] These findings show metabolism as the main mechanism of drug elimination, and extrahepatic clearance plays a lesser role in the total elimination.[51] These findings also indicate that a good prediction of the *in vivo* liver clearance would give a reasonable estimation of the total systemic clearance. Several *in vitro* models have been established for the prediction of liver clearance. Incubation with microsomes, hepatocytes or liver slices are validated techniques for the prediction of the hepatic metabolic intrinsic clearance ($Cl_{int}$), which can be scaled later to get the liver *in vivo* clearance.[57,60] In the current study, *in vitro* metabolism with Supersomes was used to predict the liver metabolism as described above. *In vitro* values were scaled to the corresponding *in vivo* values using the following assumptions: 111 pmol of CYP3A4/mg of microsomal protein; 38 mg of microsomal protein/g of liver tissue; average liver weight was assumed to be 1800 g. In the absence of an experimental value for the microsomal fraction unbound, it was assumed to be similar to the plasma unbound fraction (17.8%).

Although the contribution of other CYPs was minimal relative to CYP3A4, predicted $V_{max}$ and $K_m$ values for each CYP enzyme were estimated and included in the prediction of the total liver clearance to establish maximal simulation for the liver metabolism. It was assumed that CYP450 isoforms have similar affinity for UK-343,664 and the difference in the reported fraction metabolized after 30 min incubation was attributed to differences in the $V_{max}$. Eventually $Cl_{int}$ of UK-343,664 for each CYP was calculated using eq 3:

$$Cl_{int} = \frac{V_{max}}{K_m} \quad (3)$$

Scaling of the *in vivo* $Cl_{int}$ to the *in vivo* hepatic clearance was calculated by GastroPlus using the well stirred model with 90 L/h hepatic blood flow. Based on excretion studies, hepatic clearance was assumed to be around 90% of the total clearance, so the extrahepatic clearance was assumed to be one-ninth of the predicted hepatic clearance.

*Plasma Protein Binding and Blood-to-Plasma Concentration Ratio of UK-343,664.* Plasma protein binding of UK-343,664 has been previously reported by Abel et al.[38] The binding of UK-343,664 to human plasma proteins remained relatively constant over the concentration range 10−1000 ng/mL. The mean proportion of drug bound to protein was 82.5% at 10, 100, and 1000 ng/mL.[38] These results show that plasma protein binding is not contributing to the nonlinear behavior of the compound. Blood-to-plasma concentration ratio of the compound was predicted by the PBPKPlus module of GastroPlus.

*Building and Fitting the Pharmacokinetic Model Using GastroPlus.* Many input parameters are required to aid the prediction of the absorption and disposition of a drug after oral administration. For example, the dosage form and physicochemical properties of a drug, such as solubility at different pH values, diffusivity and lipophilicity, are very important to predict the dissolution and solublization in the GIT and the subsequent diffusion across the intestine. Physiological factors and parameters including the GI transit time, physiological pH, small intestine volume, intestinal metabolizing enzymes and transporters are also important and significantly impact the bioavailability of the drug. Good prediction of disposition pharmacokinetic parameters and the pharmacokinetic compartment model used are also important. The disposition parameters predicted from the above experiments were used to build this simulation model, and the intestinal absorption was simulated using the ACAT model.

**Gastrointestinal Absorption Model.** The ACAT model was used to simulate and predict the absorption of UK-343,664 in the small intestine. The theoretical basis and mathematical description of the CAT and the extension made in ACAT model have been described in several studies[34,48] Table 1 describes the ACAT physiological model parameters used in the simulations. Human fasted physiology model was chosen, and optimized log *D* model was applied for calculating the absorption scaling factors for the intestinal compartments.

The absorption rate in the ACAT model is a function of passive diffusion, and efflux and influx transporters distributed

**Table 2. Disposition Parameters Predicted for UK-343,664**

| parameter | value | source |
|---|---|---|
| passive permeability | $2.25 \times 10^{-4}$ cm/s | *in situ* perfusion study |
| *fu* plasma | 0.175 | Abel et al. 2001[38] |
| blood to plasma concentration ratio | 0.685 | PBPK plus |
| P-gp $V_{max}$ | 0.02 mg/s | optimized value of *in vitro* data(0.015 mg/s) |
| P-gp $K_m$ | 0.97 $\mu$g/mL | optimized value of *in vitro* data (4.1 $\mu$g/mL) |
| overall vol of distribution ($V_D$) | 2.0 L/kg | Rodgers mechanistic approach and allometric scaling from rats |
| vol of central compartment ($V_c$) | 1.13 L/kg | optimization module in GastroPlus |
| $k_{12}$ and $k_{21}$ | 0.88 and 1.23 | optimization module in GastroPlus, accounted for 0.84 L/kg in peripheral compartment |
| CYP3A4 $V_{max}$ | 2.78 mg/s | *in vitro* metabolism |
| CYP3A4 $K_m$ | 46.82 $\mu$g/mL | experimental bound $K_m$ = 465 $\mu$M converted to $\mu$g/mL and corrected to unbound $K_m$ assuming $fu_{mic}$ = 17.8% in vitro metabolism |
| CYP2C19 $V_{max}$ | 0.81 mg/s | *in vitro* metabolism |
| CYP2D6 $V_{max}$ | 0.44 mg/s | *in vitro* metabolism |
| CYP2C9 $V_{max}$ | 0.12 mg/s | *in vitro* metabolism |
| CYP2C8 $V_{max}$ | 0.19 mg/s | *in vitro* metabolism |
| CYP(2C8, 2D6, 2C9, 2C19) $K_m$ | 46.82 $\mu$g/mL | measured by Supersomes for 3A4 and applied to all other CYP450s |
| extrahepatic clearance | 0.09 L/h/kg | estimation based on excretion studies in rats and dogs. |

in each compartment. In general the total flux in each intestinal compartment can be calculated using eq 4:

$$\frac{dm}{dt} = AP_{PT}C_{lumen} + \frac{V_{max(influx)}C_{lumen}}{K_{m(influx)} + C_{lumen}} - \frac{V_{max(efflux)}C_{ent}}{K_{m(efflux)} + C_{ent}} \quad (4)$$

where $A$ is the surface area of a membrane; $P_{PT}$ is the passive permeability; $C_{ent}$ is the concentration of a drug inside the enterocytes for the efflux and $C_{lumen}$ is the luminal concentration for the influx; $K_m$ is the Michaelis−Menten constant of the compound with the influx or the efflux; $V_{max}$ is the maximum efflux or influx mediated transport.[19]

In the current study, the prediction of the permeability due to passive diffusion was calculated using the *in situ* perfusion study of UK-343,664 with verapamil (a P-gp and CYP3A4 inhibitor) in rats as described above, which was eventually scaled to the human permeability. In GastroPlus, factors such as changes in the pH, surface area and transit time are also considered by adding an absorption scaling factor for each compartment to the above equation. The contribution of efflux transport by P-gp on the absorption rate was also accounted for in building the GI absorption model, where the fitted *in vitro* values of $K_m$ and $V_{max}$ for P-gp were obtained from transport studies using Caco-2 cells, and were compared to the values used in fitting the *in vivo* nonlinear dose dependence of the gut efflux rate.

There was no evidence of the contribution of influx transporters in the preclinical studies, thus it was excluded from the model. The distribution of P-gp in the GIT is not uniform, as it was shown by many studies in both animals and human that the relative distribution of P-gp increases aborally. The ACAT model in GastroPlus accounts for the relative distribution of P-gp based on studies describing experimental distribution in human tissue.[61,62] The contribution of passive diffusion and efflux transport were integrated together to account for the total rate of absorption from the lumen to enterocytes. The contribution of intestinal metabolism was also considered in the simulation by GastroPlus to calculate the gut metabolism rate by using the *in vitro* $K_m$ and $V_{max}$ values for CYPs. In contrast to P-gp, the distribution of CYP450 decreases aborally along the GIT. The relative distribution of CYP450 was also included in the calculation of the gut metabolism rate in each compartment.[23] It is important to note that gut metabolism and apical membrane efflux will affect free drug concentration in the enterocyte, and the dynamic changes in concentration gradient will impact the rate and fraction absorbed both into and out of the enterocytes to the intestinal lumen and portal vein. Thus, the total flux rate of UK-343,664 to the portal vein in each compartment can be calculated by eq 5:

$$\frac{dm}{dt} = AP_{PT}C_{lumen} - \frac{V_{max(efflux)}C_{ent}}{K_{m(efflux)} + C_{ent}} - \frac{V_{max(CYP450)}C_{ent}}{K_{m(CYP450)} + C_{ent}} \quad (5)$$

The effect of disintegration and dissolution rate of UK-343,664 was of no significance in this study as the drug was administered as an oral solution dosage form. Hence the dissolution rate has no impact on the absorption rate; however the solubility of the compound at physiological pH values has a significant impact on the precipitation of the drug at higher pH values.

## RESULTS

**Prediction of the Disposition Model Parameters and Physicochemical Properties.** *Prediction of the Intestinal Permeability.* The $P_{eff}$ of UK-343,664 in the rat, obtained from the *in situ* studies, was found to be $0.645 \times 10^{-4}$ cm/s, which was scaled to $2.25 \times 10^{-4}$ cm/s in human. The ADMET Predictor estimated value $1.1 \times 10^{-4}$ cm/s was close to the permeability value obtained from the *in situ* perfusion study.

*Prediction of Systemic Clearance.* The systemic clearance was predicted and scaled from CYP3A4 Supersomes, assuming major systemic clearance by the liver as suggested from the excretion studies reported by Walker et al. 2001.[51] The *in vitro*

$K_m$ and $V_{max}$ were found to be 465 $\mu$M and 38.9 pmol/min/pmol CYP3A4 protein, respectively. These values were scaled to the *in vivo* values using the assumptions described above. The scaled $V_{max}$ and $K_m$ values for CYP enzymes are presented in Table 2. These scaled *in vivo* $K_m$ and $V_{max}$ for the CYP enzymes were used to simulate the liver clearance assuming well stirred model. The extrahepatic clearance was predicted to be 0.09 L/h/kg by renal clearance, which presents one-ninth of the liver clearance based on the excretion studies,[51] thus 0.09 L/h/kg value was used in the simulation. The plasma fraction of unbound drug ($fu$) was determined and found to be 17.5% and was used in the simulation.[51] Blood/plasma drug ratio was predicted by the PBPKPlus module of GastroPlus, and it was estimated to be 0.685.

*Prediction of Volume of Distribution ($V_D$).* To determine the $V_D$ in rats, 37.5 mg/kg dose of UK-343,664 was intravenously administered ($n$ = 3). Blood samples were collected and drug concentrations were determined as indicated above. Plasma concentration vs time profile was plotted using the PKPlus module of GastroPlus. The obtained $V_D$ of UK-343,664 in rats was 0.5 L/kg. In human, $V_D$ was calculated using the PBPKPlus module in GastroPlus which used Rodgers mechanistic equations, and by the allometric scaling from the rat value for $V_D$ after correction for differences in protein binding. The fraction unbound in rats and human was 0.046 and 0.17, respectively.[38,51] Allometric scaling from rats resulted in a $V_D$ value of 2 L/kg. $V_D$ calculated by Rodgers mechanistic equations was comparable to that obtained by the allometric scaling method and equals 2 L/kg, which was used for all the simulations. *In vivo* data in humans and rats showed a two compartmental behavior. In addition, distribution behavior of UK-343,664 obtained by PBPK modeling using the Kpu values obtained using Rodgers mechanistic equation suggested also a two compartmental behavior of UK-343,664. *In vivo* data in humans and iv studies in rats fitted a two compartment behavior of the UK compound. $k_{12}$ and $k_{21}$ values were fitted based on the *in vivo* data (Table 2).

*Intestinal P-gp and CYP3A4 Pharmacokinetic Constants.* The *in vitro* $K_m$ and $V_{max}$ for the metabolism of UK-343,664 by CYP3A4 were 465 $\mu$M and 38.9 pmol/min/pmol protein, respectively. For P-gp, the *in vitro* $V_{max}$ and $K_m$ values were 0.015 mg/s and 4.13 $\mu$g/mL respectively, while the optimized $V_{max}$ and $K_m$ resulted in values of 0.0201 mg/s and 0.97 $\mu$g/mL, respectively. Finding a fitted value of $K_m$ for P-gp in the *in vivo* simulation that is significantly lower than the *in vitro* value and also explains the observed nonlinear dose dependence is not unusual.[34] One reason for the difference between the *in vitro* value of $K_m$ for interaction with the binding site of P-gp and the fitted *in silico* value is due to difference in simulated concentration in the cytoplasm of the enterocyte compared to the concentrations in the cell culture supernatant used *in vitro*. The binding sites for P-gp lie within the apical membrane of the enterocytes where P-gp substrates are thought to enter the membrane and diffuse laterally for interaction with P-gp or by direct interaction with intracellular sites. As a result, P-gp saturation in this simulation will be a function of the cytoplasm concentration, which is assumed to be much lower than the *in vitro* apparent $K_m$.[63,64] $V_{max}$ and $K_m$ values for CYP3A4, CYP2D6 and P-gp were used in the ACAT physiology along with their relative distribution in the gut. The $K_m$ value for the P-gp in the intestine was reduced to 0.97 $\mu$g/mL. Results for P-gp and CYP pharmacokinetic constants are presented in Table 2.

*Dosage Form and Physicochemical Properties.* The drug was administered as a solution dosage form, thus the particle size and the dissolution of UK-343,664 are not contributing factors to the absorption process. However, the pH−solubility profile is important to investigate the precipitation of UK-343,664 at different pH values in different segments of the GIT. Literature data for the basic p$K_a$ value of the compound (6.9) was used in the simulation. Solubility of UK-343,664 at pH 5, 6.8, 7.4, and 8 was estimated using the shake flask method as presented above. The solubility was 9 mg/mL at pH 5, and 0.1 mg/mL at pH 6.8, 7.4, and 8. The rest of the physicochemical properties were obtained from the literature or estimated by ADMET Predictor. A summary of these properties is presented in Table 3.

**Table 3. Physicochemical Properties and Dosage Form Parameters of UK-343,664 Used in the Simulation**

| parameter | value | source |
|---|---|---|
| mol formula | $C_{28}H_{35}N_7O_4S$ | Walker et al. 2001[51] |
| mol wt | 565.7 g/mol | Walker et al. 2001[51] |
| base p$K_a$ | 6.9 | Walker et al. 2001[51] |
| ref log $D$ | 3.1 | Walker et al. 2001[51] |
| solubility at pH 5 | 9 mg/mL | solubility studies |
| solubility at pH 6.8 | 0.1 mg/mL | solubility studies |
| solubility at pH 7.4 | 0.1 mg/mL | solubility studies |
| solubility at pH 8 | 0.1 mg/mL | solubility studies |
| dosage form | 0.1 N HCl aq soln | Abel et al. 2001[38] |
| initial dose | 30, 100, 200, 400, 800 mg | Abel et al. 2001[38] |
| dose vol | 250 mL | Abel et al. 2001[38] |
| mean precip time | 900 s | GastroPlus |
| diffusion coeff | $0.569 \times 10^{-5}$ | GastroPlus |

**Simulation of Nonlinear Dose Dependence of UK-343,664.** The physicochemical and disposition parameters predicted above (Table 2) were integrated to build the simulation model. Eventually, simulation trials for the prediction of bioavailability and plasma concentration vs time profiles for the dose escalating study in human using the predicted disposition parameters were performed for 30, 100, 200, 400, 800 mg using GastroPlus. All doses were simulated using the same pharmacokinetic parameters and the same set of $K_m$ and $V_{max}$ values for P-gp and CYP450. Simulation trials were successfully able to predict the nonlinear pharmacokinetic profiles for the dose escalating studies in human. Comparison of the simulation results with the experimental plasma pharmacokinetic profiles is presented in Figure 2. The predicted pharmacokinetic profiles were similar to the observed profiles, and the goodness of fit was tested by correlating the observed data with the predicted data at all time points across the 30, 100, 200, 400, 800 mg doses. The correlation coefficient was greater than 0.8 for all doses. In addition, the relative mean absolute error (calculate as MAE/$C_{max}$ × 100) were as low as 5.6, 11.8, 8.4, 5.7, and 10.7% for 30, 100, 200, 400, and 800 mg dose, respectively. This *in silico* model could also generate accurate estimates for AUC, $C_{max}$ and $T_{max}$. The predicted values for $C_{max}$ and AUC lie within one standard deviation of the mean experimental parameters. Figures 3A and 3B demonstrate predicted AUC and $C_{max}$ values comparable to those observed experimentally at different doses of the compound. For example, the simulation trials resulted in AUC values ranging from 37 to 7,412 ng h mL$^{-1}$ compared to the observed values 37 ± 9.3 and 10,607 ± 3,335 ng h mL$^{-1}$ in

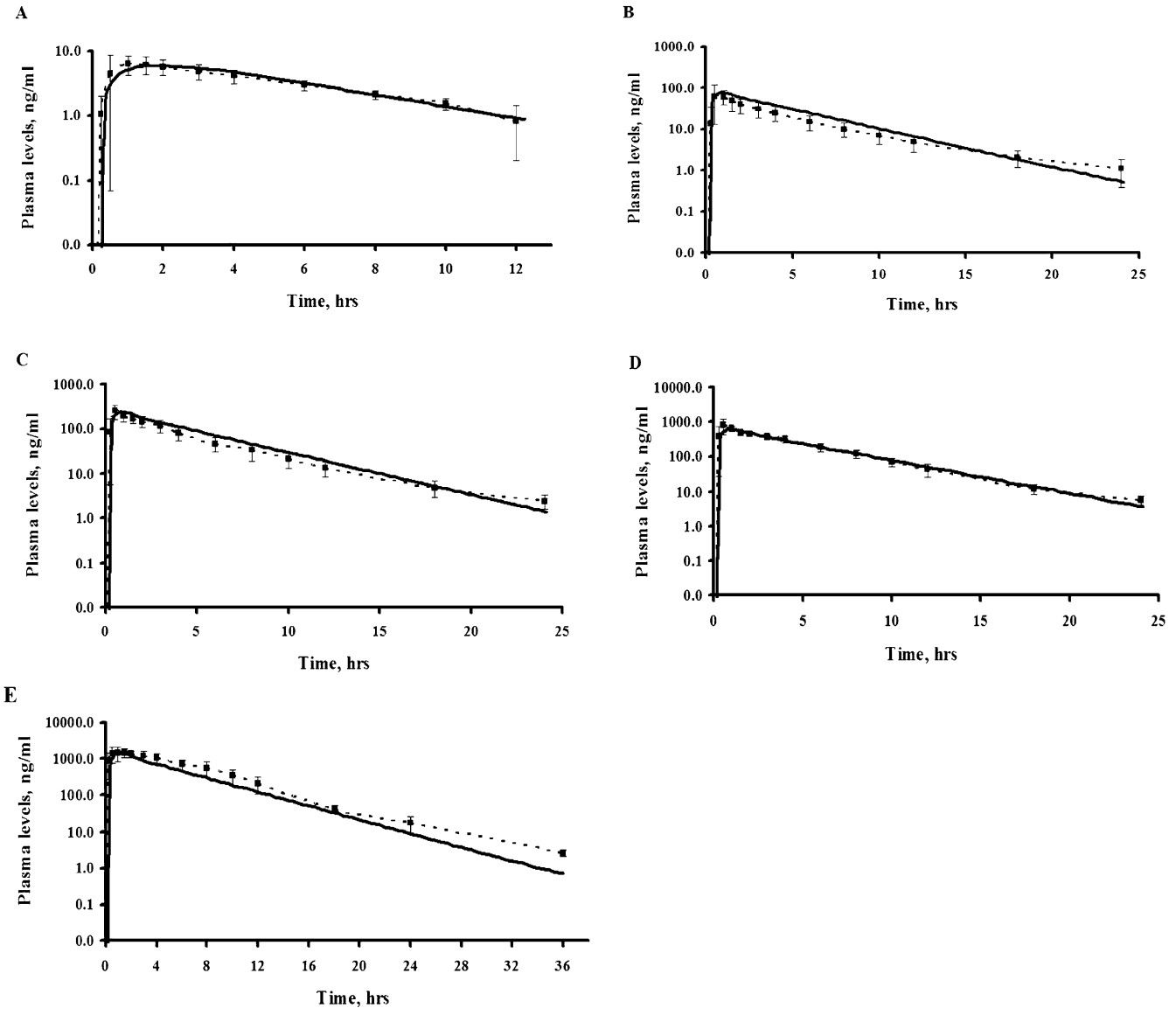


**Figure 2.** Mean plasma concentration vs time profiles in human male volunteers following the administration of a single oral dose of (A) 30, (B) 100, (C) 200, (D) 400, and (E) 800 mg of UK-343,664, obtained experimentally (- - -), or simulated using GastroPlus (—).

the dose range examined. In the case of linear pharmacokinetics this relationship should be a straight line and when a saturable process is involved, such as in the case of saturation of efflux mechanisms or metabolism, the line deviates from linearity as observed with the compound UK-343,664 (Figure 3). The predicted bioavailability values also showed an increase in the fraction reaching the systemic circulation with increasing the dose where the bioavailability was predicted to be 5.4, 14.8, 22.4, 29.4, and 35.2% for 30, 100, 200, 400, 800 mg dose, respectively (Figure 3C). Table 4 compares the predicted vs observed AUC, $C_{max}$ and $T_{max}$. Furthermore, this model could also give a successful prediction of the reported oral clearance (CL/F) at 30 mg dose which was approximately 150 mL/min/kg.[38] Moreover, the simulated $AUC_{0-t}$, $C_{max}$, and $T_{max}$ (9.5 ng h $mL^{-1}$, 1.3 ng/mL, and 2.5 h, respectively) for a 10 mg dose was comparable to their reported mean values of only five subjects (5.6 ± 5.2 ng h $mL^{-1}$, 1.3 ± 0.3 ng/mL, 3.5 ± 1.7 h, respectively).[38]

In order to assess the combined effect of variation in the predicted disposition parameters that were assumed to be the contributing factors to the nonlinear kinetics (i.e., P-gp and CYP450), a stochastic simulation was performed using the virtual trial feature in GastroPlus. The coefficient of variation (CV%) values used in this simulation were selected based on our experience with the accuracy of the predicted disposition parameters governing the absorption process. This trial was done for 24 virtual patients, which is the same number of volunteers used in the *in vivo* study,[38] and random samples of all the variables were generated for each simulation. The following parameters and CV% were used in the trial:

P-gp ($V_{max}$ and $K_m$), CV% = 50%

CYP450 ($V_{max}$ and $K_m$), CV% = 50%

Simulation results for the 400 mg dose are shown in Figure 4. The figure shows the mean experimental concentration vs time profile with the corresponding standard deviation for each time point. The green shaded area in the figure represents the 90% confidence interval (CI) around the mean. Almost all of the experimental clinical observations lie within 90% CI of the


dx.doi.org/10.1021/mp200275j | *Mol. Pharmaceutics* 2012, 9, 492–504

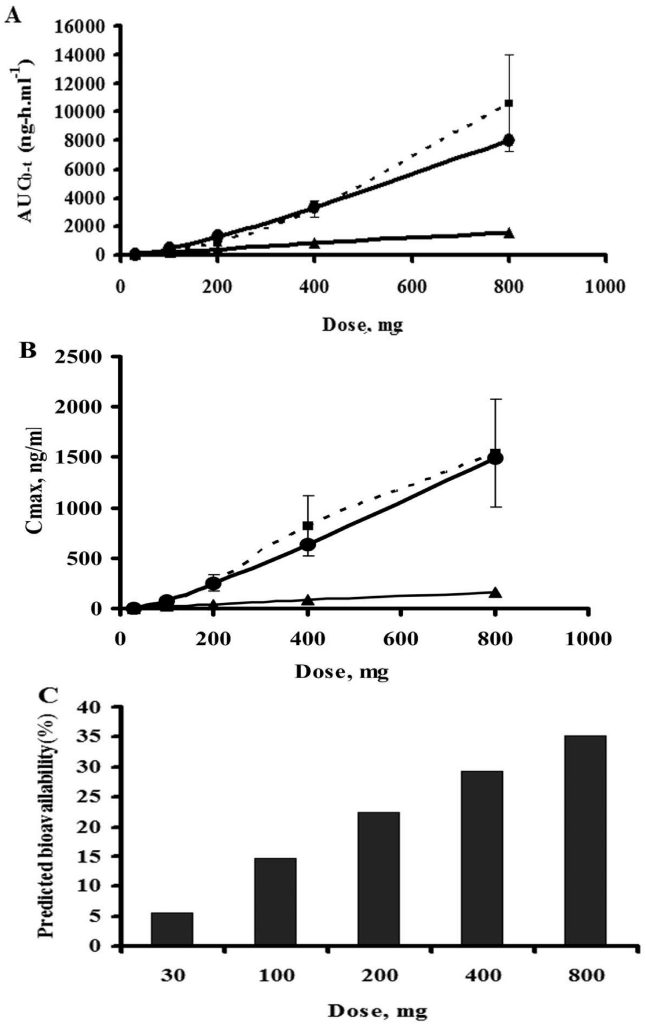


**Figure 3.** Nonlinear increase in $AUC_{0\text{-}t}$ (A), and $C_{max}$ (B) as a function of dose as predicted by GastroPlus (●), or experimentally observed (■) following the oral administration of a single dose of UK-343,664 to human subjects. In linear kinetics the increase in $AUC_{0-t}$ and $C_{max}$ is expected to be proportional to the increase in the dose (▲). (C) Predicted increase in the UK-343,664 bioavailability as a function of time.

simulation, which further supports the validity of the *in silico* model. In addition, all of the observed concentration vs time profiles are contained within the 100% probability plot (blue color). The results of this stochastic simulation could successfully cover the variation of the observed data points.

## DISCUSSION

As previously stated, UK-343,664 showed a nonlinear pharmacokinetic behavior where a 247- and a 287-fold increase in the AUC and $C_{max}$, respectively, were observed over the 27-fold increase in the dose range. This nonlinear behavior was accurately predicted with our *in silico* model despite the complex factors governing the absorption and the elimination of UK-343,664.

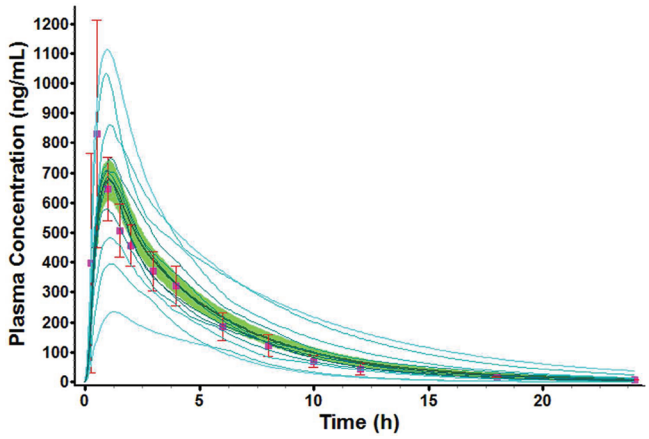


**Figure 4.** Virtual trial simulation for 24 subjects following an oral dose of 400 mg. Solid line represents the mean of 24 simulations. Squares with error bars represent the observed clinical plasma concentrations vs time profiles. The green shaded area represents the 90% confidence interval for the simulated data and the solid blue, dashed, and dotted lines represent individual simulated results that include 100, 95, 90, 75, 50, 25, and 10% of the range of simulated data.

The fixed $T_{1/2}$ values obtained from the experimental data at different doses suggested that the nonlinearity is not attributed to the saturation of the systemic clearance.[38] Furthermore, the fixed value for the protein binding across different concentrations in the plasma protein study suggests that protein binding does not contribute to the nonlinear behavior observed.[38] Given this information, it was assumed that the nonlinear behavior of UK-343,664 is mostly attributed to a saturable absorption process. The *in vivo* studies showed an increase in the $T_{max}$ from 3.5 h at a 10 mg dose compared to 1.2 h at higher doses, which suggests the GIT acting as an absorption barrier at low doses.[38] This conclusion was supported by the *in vitro* and the *in situ* preclinical studies, which confirmed UK-343,664 as a substrate with high affinity for P-gp, a major efflux transporter in the GIT.[50] The *in situ* intestinal perfusion studies showed a significant increase in the permeability of the UK-343,664 with increasing the perfusion concentration, suggesting the involvement of a saturable efflux transporter governing the absorption rate of the compound.[50] However, the low $K_m$ of the UK-343,664 for P-gp means that the transporter will be saturated quickly; as a result there should be another saturable absorption process explaining the nonlinearity across the wide dose range 10−800 mg of UK-343,664.

**Table 4. Simulation Results for Oral Solution Formulations Containing 30, 100, 200, 400, and 800 mg of UK-343,664**

| | $AUC_{0-t}$ ng h $mL^{-1}$ | | $C_{max}$, ng/mL | | $T_{max}$, h | |
|---|---|---|---|---|---|---|
| dose (mg) | obsd | predicted | obsd | predicted | obsd | predicted |
| 30 | 37.3 ± 9.3 | 38 | 7.1 ± 2.8 | 6 | 1.2 ± 0.5 | 1.8 |
| 100 | 280 ± 116 | 387 | 78 ± 42 | 77 | 0.8 ± 0.4 | 0.9 |
| 200 | 940 ± 271 | 1166 | 255 ± 86 | 243 | 0.6 ± 0.2 | 0.9 |
| 400 | 3,166 ± 581 | 3,084 | 903 ± 300 | 639 | 0.6 ± 0.3 | 1 |
| 800 | 10,067 ± 3335 | 7,412 | 1,743 ± 535 | 1,500 | 1.2 ± 0.7 | 1.1 |


dx.doi.org/10.1021/mp200275j | *Mol. Pharmaceutics* 2012, 9, 492−504

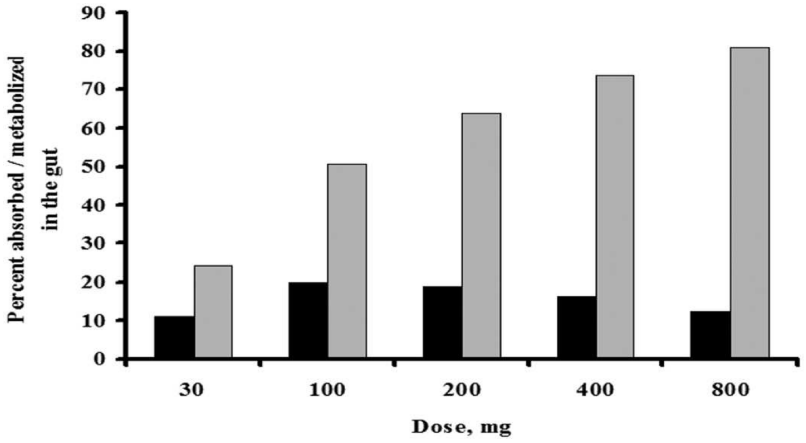


**Figure 5.** The predicted fraction absorbed (gray columns), and the fraction metabolized of UK-343,664 following the administration of a single oral dose of 30, 100, 200, 400, 800 mg.

The saturable metabolism by intestinal CYP3A4 has also been suggested as a contributor to the nonlinear absorption kinetics of UK-343,664. The *in vitro* studies have shown that UK-343,664 has a high intrinsic clearance value by CYP3A4, which is a major intestinal metabolizing enzyme. In addition, the analysis of the feces in excretion studies in rats and dogs showed a very high recovery of UK-343,664 metabolite.[51] The involvement of intestinal metabolism was confirmed when Kaddoumi and colleagues (2006) detected up to 10% intestinal metabolism of UK-343,664 by *in situ* perfusion studies.[50] The 6-fold increase in the proportion of UK-343,664 excreted unchanged in the urine of human volunteers in the clinical studies over the dose range 10−800 mg is consistent with our assumption that saturable intestinal processes are contributing to the nonlinear intestinal absorption of UK-343,664.[38] CYP3A4 and P-gp may also act in concert to decrease the intestinal absorption which further complicates the absorption process. The contribution of P-gp to the absorption process can be shown by the change in the fraction absorbed across the administered doses because the fraction absorbed in GastroPlus is the fraction of drug crossing the apical membrane of the enterocyte; as a result it is a function of interaction between passive diffusion and efflux transporters. Any increase in the fraction absorbed across the administered doses will result in a nonlinear absorption and a supraproportional increase in the AUC due to saturation of P-gp. Figure 5 shows the increase in the fraction absorbed across the administered doses, which confirms the contribution of P-gp in the nonlinear pharmacokinetics. In addition, the fraction of dose metabolized by the gut is shown in the same figure (Figure 5), which illustrates a definite peak at a dose of 100 mg. These results demonstrate a general decrease in the fraction metabolized by the gut with increasing the dose from 100 to 800 mg, which results in an increase in the fraction reaching the portal vein and eventually the systemic circulation (Table 5). Interestingly, the pharmacokinetic model showed that the fraction metabolized in the gut at the lowest dose (30 mg) is less than the fraction metabolized by the gut at 100 mg. This low level of gut extraction at a 30 mg dose could be attributed to the efficient efflux and protective influence of P-gp that results in intraenterocyte unbound concentrations below the true intracellular $K_m$ for P-gp. Therefore, P-gp minimizes the exposure to metabolizing enzymes in the upper GIT at low doses. In addition, at this dose P-gp will delay the absorption of the drug

**Table 5. Comparison of the Effect of Virtual P-gp Knockout of Intestinal Metabolism on the Predicted Percent Absorbed (Fa), Percent of Dose Extracted in the Gut ($E_{gut}$ = Fa − FDp), Percent of Mass Absorbed That Is Extracted by Gut ($E_{ma}$ = (1 − (FDp/Fa) × 100), Percent Reaching Portal Vein (FDp), and Bioavailability ($F$)**

| dose (mg) | Fa | $E_{gut}$ | $E_{ma}$ | FDp | $F$ |
|---|---|---|---|---|---|
| Simulations with P-gp and Gut Metabolism | | | | | |
| 30 | 22.2 | 11.5 | 51.8 | 10.7 | 5.5 |
| 100 | 48.2 | 19.5 | 40.5 | 28.7 | 14.8 |
| 200 | 62.1 | 19 | 30.6 | 43.1 | 22.4 |
| 400 | 72.8 | 16.3 | 22.4 | 56.5 | 29.4 |
| 800 | 80.3 | 12.8 | 15.9 | 67.5 | 35.2 |
| Simulations without P-gp | | | | | |
| 30 | 99.9 | 46.3 | 46.3 | 53.6 | 27.7 |
| 100 | 99.9 | 37.5 | 37.5 | 62.4 | 32.3 |
| 200 | 99.9 | 30.7 | 30.7 | 69.2 | 35.9 |
| 400 | 99.9 | 23.8 | 23.8 | 76.1 | 39.6 |
| 800 | 99.9 | 17.7 | 17.7 | 82.2 | 42.8 |
| Simulations without Gut Metabolism | | | | | |
| 30 | 12.3 | 0 | 0 | 12.3 | 6.2 |
| 100 | 41.3 | 0 | 0 | 41.3 | 21.3 |
| 200 | 57.3 | 0 | 0 | 57.3 | 29.6 |
| 400 | 69.7 | 0 | 0 | 69.7 | 36.1 |
| 800 | 78.4 | 0 | 0 | 78.4 | 40.8 |

to the lower segments of the GIT where the expression level of CYP3A4 is significantly lower. It can be concluded from Figure 5 that both P-gp and intestinal metabolism contribute to the increase in the fraction reaching systemic circulation and hence to the nonlinear absorption kinetics. Our observation of the protective effect of P-gp at doses that result in enterocyte concentrations below the $K_m$ is consistent with the views expressed by Thakker.[51] In order to identify the main contributor (P-gp or CYP3A4) to the nonlinear behavior, and compare the significance of contribution of P-gp and CYP3A4 to the absorption process, the increase in fraction absorbed and the decrease in fraction metabolized between each consecutive dose were compared to the increase in the fraction reaching the portal vein and to the increase in the predicted bioavailability (Figure 6, Table 5). In the absence of nonlinear intestinal absorption kinetics, the change in the fraction reaching the portal vein and the change in the fraction metabolized in the intestine should collapse to zero (Figure 6);


dx.doi.org/10.1021/mp200275j | *Mol. Pharmaceutics* 2012, 9, 492−504

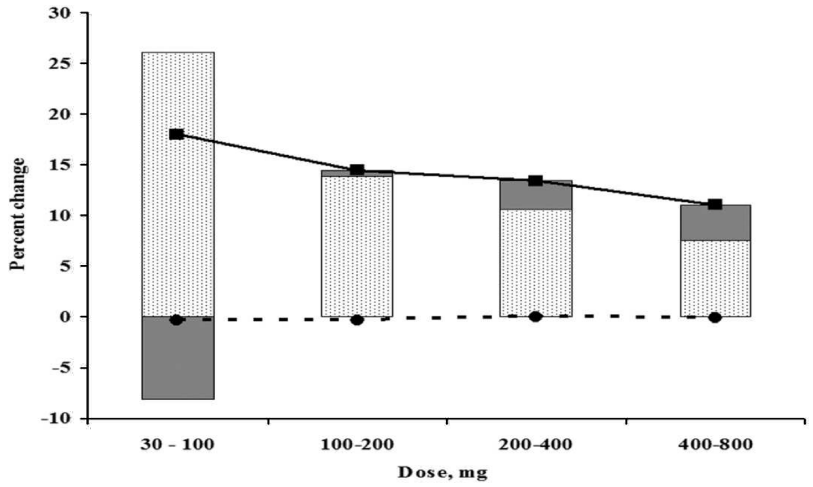


**Figure 6.** Comparison of the combined effect of the increase in the fraction absorbed (dotted columns) and the decrease in the fraction metabolized (gray columns) on the increase in fraction reaching the portal vein (■) at each consecutive dose range of UK-343,664. The change in the first pass liver metabolism is represented by ●.

however the results showed that both metabolism and P-gp are contributing to the nonlinear absorption kinetics. It can also be concluded from Figure 6 that P-gp is the main contributor to the change in the bioavailability at lower doses compared to the effect of intestinal metabolism. This is because the increase in the fraction absorbed is more significant at low doses as P-gp becomes saturated; however at higher doses the effect of P-gp represented by the effect of change of the fraction absorbed is decreased, and the change in the fraction metabolized by the intestine becomes more significant in the nonlinear pharmacokinetics. These observations suggest that the low $K_m$ value of P-gp compared to CYP3A4 results in earlier saturation of the P-gp at low doses followed by saturation of CYP3A4 at higher doses. This conclusion is supported by the observation that the $T_{max}$ of the UK-343,664 was significantly delayed only at low doses compared to higher doses.[38] It is important to realize also that the effect of liver metabolism did not contribute to the nonlinear kinetics as the hepatic metabolism was constant across the administered doses, and as a result liver first pass metabolism was 48% at all doses. This effect can be attributed to the high plasma protein binding and low levels of unbound liver concentration below the $K_m$ value of CYP3A4.

To better understand the interaction mechanism between P-gp and CYP3A4, simulation trials were performed by virtual knockout of either the intestinal P-gp or the intestinal metabolism. Then, the predicted fraction absorbed, the fraction metabolized in the intestine, the fraction reaching the portal vein, and the bioavailability were compared. Results of these simulation trials are presented in Table 5. The simulation trials following the virtual knockout of intestinal P-gp resulted in complete absorption of the drug into the enterocytes at all doses, and resulted in an increase in the intestinal fraction of dose metabolized as more drug was exposed to metabolism. However, there was a gradual decrease in the fraction of dose metabolized, from 46.3 to 17.7%, as a function of increasing dose (30−800 mg), a trend that is very different from that when P-gp was involved in the absorption process. The reason for this difference in the fraction of dose metabolized is mainly because of the difference in the fraction absorbed across the administered doses as a result of P-gp. If we calculate the percent of mass metabolized from the mass absorbed rather than from the administered dose for both cases (i.e., with and without P-gp), a similar pattern in the fraction metabolized will be observed. It is important to note that the fraction metabolized (when calculated from the fraction absorbed) is a little higher when P-gp is involved as a result of the higher exposure to P-gp as suggested by Benet.[31]

Interestingly, knocking out the intestinal metabolism resulted in a significant decrease in the fraction of dose absorbed at a 30 mg dose (12.3% compared to 22.2%, Table 5). This decrease is mostly attributed to the fact that without the metabolic contribution of CYP3A4 the intraenterocyte concentration will be higher making less of a sink effect and decreasing fraction absorbed. However, the fraction of dose reaching the portal vein is not significantly changed at a 30 mg dose by the 3A4 virtual knockout. These findings were previously suggested by Tam (2003).[46]

In addition to the intestinal P-gp and CYP3A4 interplay, the effect of solubility proved to play a very important role in the nonlinear absorption behavior of UK-343,664. The delay in absorption of UK-343,664 by P-gp caused accumulation of the drug in the lower GIT, which has a more basic microenvironment, resulting in precipitation thus hindering the absorption of the drug at this region. If precipitation in the lower GIT did not occur, a pharmacokinetic profile similar to that observed with saquinavir will be expected.[48] The long residence time in the colon would result in the formation of a second peak at a delayed time point as a result of its absorption from this region.[48]

In conclusion, this study demonstrated that intestinal P-gp efflux transporter and CYP3A4 metabolism are major contributors to the complex nonlinear absorption kinetic behavior of UK-343,664, and such behavior was successfully predicted using GastroPlus. We have also provided simulation results that explain and support the observations of both Thakker and Benet.

## ■ AUTHOR INFORMATION

### Corresponding Author

*University of Louisiana at Monroe, College of Pharmacy, 1800 Bienville Dr., Monroe, LA 71201. Phone: (318) 342-1460. Fax: (318) 342-1737. E-mail: kaddoumi@ulm.edu.

## ■ ABBREVIATIONS USED

CYP3A4, cytochrome P450 3A4; P-gp, P- glycoprotein; ACAT model, advanced compartmental absorption and transit model; $CL_{int}$, intrinsic clearance; $P_{eff}$, effective permeability; *fu*, drug fraction unbound; $V_D$, volume of distribution

## ■ REFERENCES


(1) Hidalgo, I. J. Assessing the absorption of new pharmaceuticals. *Curr. Top. Med. Chem.* **2001**, *1* (5), 385−401.

(2) Levet-Trafit, B.; Gruyer, M. S.; Marjanovic, M.; Chou, R. C. Estimation of oral drug absorption in man based on intestine permeability in rats. *Life Sci.* **1996**, *58* (24), PL359−PL363.

(3) Chan, K. K.; Gibaldi, M. Evaluating drug absorption after oral administration. Some problems and some solutions. *Eur. J. Clin. Pharmacol.* **1984**, *26* (2), 255−259.

(4) Burton, P. S.; Goodwin, J. T.; Vidmar, T. J.; Amore, B. M. Predicting drug absorption: how nature made it a difficult problem. *J. Pharmacol. Exp. Ther.* **2002**, *303* (3), 889−895.

(5) Benet, L. Z. Predicting drug disposition via application of a Biopharmaceutics Drug Disposition Classification System. *Basic Clin. Pharmacol. Toxicol.* **2010**, *106* (3), 162−167.

(6) Hurst, S.; Loi, C. M.; Brodfuehrer, J.; El-Kattan, A. Impact of physiological, physicochemical and biopharmaceutical factors in absorption and metabolism mechanisms on the drug oral bioavailability of rats and humans. *Expert Opin. Drug Metab. Toxicol.* **2007**, *3* (4), 469−489.

(7) Abuzarur-Aloul, R.; Gjellan, K.; Sjolund, M.; Graffner, C. Critical dissolution tests of oral systems based on statistically designed experiments. III. In vitro/in vivo correlation for multiple-unit capsules of paracetamol based on PLS modeling. *Drug Dev. Ind. Pharm.* **1998**, *24* (4), 371−383.

(8) Fujioka, Y.; Kadono, K.; Fujie, Y.; Metsugi, Y.; Ogawara, K.; Higaki, K.; Kimura, T. Prediction of oral absorption of griseofulvin, a BCS class II drug, based on GITA model: utilization of a more suitable medium for in-vitro dissolution study. *J. Controlled Release* **2007**, *119* (2), 222−228.

(9) Takano, R.; Furumoto, K.; Shiraki, K.; Takata, N.; Hayashi, Y.; Aso, Y.; Yamashita, S. Rate-limiting steps of oral absorption for poorly water-soluble drugs in dogs; prediction from a miniscale dissolution test and a physiologically-based computer simulation. *Pharm. Res.* **2008**, *25* (10), 2334−2344.

(10) He, X.; Sugawara, M.; Kobayashi, M.; Takekuma, Y.; Miyazaki, K. An in vitro system for prediction of oral absorption of relatively water-soluble drugs and ester prodrugs. *Int. J. Pharm.* **2003**, *263* (1−2), 35−44.

(11) Zhao, Y. H.; Abraham, M. H.; Le, J.; Hersey, A.; Luscombe, C. N.; Beck, G.; Sherborne, B.; Cooper, I. Rate-limited steps of human oral absorption and QSAR studies. *Pharm. Res.* **2002**, *19* (10), 1446−1457.

(12) Kobayashi, M.; Sada, N.; Sugawara, M.; Iseki, K.; Miyazaki, K. Development of a new system for prediction of drug absorption that takes into account drug dissolution and pH change in the gastrointestinal tract. *Int. J. Pharm.* **2001**, *221* (1−2), 87−94.

(13) Ribadeneira, M. D.; Aungst, B. J.; Eyermann, C. J.; Huang, S. M. Effects of structural modifications on the intestinal permeability of angiotensin II receptor antagonists and the correlation of in vitro, in situ, and in vivo absorption. *Pharm. Res.* **1996**, *13* (2), 227−233.

(14) Zhao, Y. H.; Le, J.; Abraham, M. H.; Hersey, A.; Eddershaw, P. J.; Luscombe, C. N.; Butina, D.; Beck, G.; Sherborne, B.; Cooper, I.; Platts, J. A. Evaluation of human intestinal absorption data and subsequent derivation of a quantitative structure-activity relationship (QSAR) with the Abraham descriptors. *J. Pharm. Sci.* **2001**, *90* (6), 749−784.

(15) Oostendorp, R. L.; Beijnen, J. H.; Schellens, J. H. The biological and clinical role of drug transporters at the intestinal barrier. *Cancer Treat. Rev.* **2009**, *35* (2), 137−147.

(16) Shirasaka, Y.; Sakane, T.; Yamashita, S. Effect of P-glycoprotein expression levels on the concentration-dependent permeability of drugs to the cell membrane. *J. Pharm. Sci.* **2008**, *97* (1), 553−565.

(17) del Amo, E. M.; Heikkinen, A. T.; Monkkonen, J. In vitro-in vivo correlation in P-glycoprotein mediated transport in intestinal absorption. *Eur. J. Pharm. Sci.* **2009**, *36* (2−3), 200−211.

(18) Lennernas, H. Intestinal permeability and its relevance for absorption and elimination. *Xenobiotica* **2007**, *37* (10−11), 1015−1051.

(19) Sugano, K.; Kansy, M.; Artursson, P.; Avdeef, A.; Bendels, S.; Di, L.; Ecker, G. F.; Faller, B.; Fischer, H.; Gerebtzoff, G.; Lennernaes, H.; Senner, F. Coexistence of passive and carrier-mediated processes in drug transport. *Nat. Rev. Drug Discovery* **2010**, *9* (8), 597−614.

(20) Nakanishi, Y.; Matsushita, A.; Matsuno, K.; Iwasaki, K.; Utoh, M.; Nakamura, C.; Uno, Y. Regional distribution of cytochrome p450 mRNA expression in the liver and small intestine of cynomolgus monkeys. *Drug Metab. Pharmacokinet.* **2010**, *25* (3), 290−297.

(21) Kagan, L.; Dreifinger, T.; Mager, D. E.; Hoffman, A. Role of p-glycoprotein in region-specific gastrointestinal absorption of talinolol in rats. *Drug Metab. Dispos.* **2010**, *38* (9), 1560−1566.

(22) Ingelfinger, F. J. Regional absorption. *Am. J. Surg.* **1967**, *114* (3), 388−392.

(23) Paine, M. F.; Khalighi, M.; Fisher, J. M.; Shen, D. D.; Kunze, K. L.; Marsh, C. L.; Perkins, J. D.; Thummel, K. E. Characterization of interintestinal and intraintestinal variations in human CYP3A-dependent metabolism. *J. Pharmacol. Exp. Ther.* **1997**, *283* (3), 1552−1562.

(24) Kalitsky-Szirtes, J.; Shayeganpour, A.; Brocks, D. R.; Piquette-Miller, M. Suppression of drug-metabolizing enzymes and efflux transporters in the intestine of endotoxin-treated rats. *Drug Metab. Dispos.* **2004**, *32* (1), 20−27.

(25) Cong, D.; Doherty, M.; Pang, K. S. A new physiologically based, segregated-flow model to explain route-dependent intestinal metabolism. *Drug Metab. Dispos.* **2000**, *28* (2), 224−235.

(26) Paine, M. F.; Davis, C. L.; Shen, D. D.; Marsh, C. L.; Raisys, V. A.; Thummel, K. E. Can oral midazolam predict oral cyclosporine disposition? *Eur. J. Pharm. Sci.* **2000**, *12* (1), 51−62.

(27) Bouer, R.; Barthe, L.; Philibert, C.; Tournaire, C.; Woodley, J.; Houin, G. The roles of P-glycoprotein and intracellular metabolism in the intestinal absorption of methadone: in vitro studies using the rat everted intestinal sac. *Fundam. Clin. Pharmacol.* **1999**, *13* (4), 494−500.

(28) Stephens, R. H.; O'Neill, C. A.; Warhurst, A.; Carlson, G. L.; Rowland, M.; Warhurst, G. Kinetic profiling of P-glycoprotein-mediated drug efflux in rat and human intestinal epithelia. *J. Pharmacol. Exp. Ther.* **2001**, *296* (2), 584−591.

(29) Sun, H.; Pang, K. S. Permeability, transport, and metabolism of solutes in Caco-2 cell monolayers: a theoretical study. *Drug Metab. Dispos.* **2008**, *36* (1), 102−123.

(30) Knight, B.; Troutman, M.; Thakker, D. R. Deconvoluting the effects of P-glycoprotein on intestinal CYP3A: a major challenge. *Curr. Opin. Pharmacol.* **2006**, *6* (5), 528−532.

(31) Benet, L. Z. The drug transporter-metabolism alliance: uncovering and defining the interplay. *Mol. Pharmaceutics* **2009**, *6* (6), 1631−1643.

(32) Darwish, M.; Kirby, M.; Robertson, P. Jr.; Tracewell, W.; Jiang, J. G. Absolute and relative bioavailability of fentanyl buccal tablet and oral transmucosal fentanyl citrate. *J. Clin. Pharmacol.* **2007**, *47* (3), 343−350.

(33) Zhang, Y.; Benet, L. Z. The gut as a barrier to drug absorption: combined role of cytochrome P450 3A and P-glycoprotein. *Clin. Pharmacokinet.* **2001**, *40* (3), 159−168.

(34) Tubic, M.; Wagner, D.; Spahn-Langguth, H.; Bolger, M. B.; Langguth, P. In silico modeling of non-linear drug absorption for the P-gp substrate talinolol and of consequences for the resulting pharmacodynamic effect. *Pharm. Res.* **2006**, *23* (8), 1712−1720.

(35) Thompson, K. L.; Vincent, S. H.; Miller, R. R.; Colletti, A. E.; Alvaro, R. F.; Wallace, M. A.; Feeney, W. P.; Chiu, S. H. Pharmacokinetics and disposition of the oxytocin receptor antagonist

L-368,899 in rats and dogs. *Drug Metab. Dispos.* **1997**, *25* (10), 1113−1118.
(36) Umehara, K. I.; Nakamata, T.; Suzuki, K.; Noguchi, K.; Usui, T.; Kamimura, H. Pharmacokinetics of YK754, a novel If channel inhibitor in rats, dogs and humans. *Eur. J. Drug Metab. Pharmacokinet.* **2008**, *33* (2), 117−127.
(37) Chan, L. M.; Lowes, S.; Hirst, B. H. The ABCs of drug transport in intestine and liver: efflux proteins limiting drug absorption and bioavailability. *Eur. J. Pharm. Sci.* **2004**, *21* (1), 25−51.
(38) Abel, S.; Beaumont, K. C.; Crespi, C. L.; Eve, M. D.; Fox, L.; Hyland, R.; Jones, B. C.; Muirhead, G. J.; Smith, D. A.; Venn, R. F.; Walker, D. K. Potential role for P-glycoprotein in the non-proportional pharmacokinetics of UK-343,664 in man. *Xenobiotica* **2001**, *31* (8−9), 665−676.
(39) Huang, W.; Lee, S. L.; Yu, L. X. Mechanistic approaches to predicting oral drug absorption. *AAPS J.* **2009**, *11* (2), 217−224.
(40) Kuentz, M.; Nick, S.; Parrott, N.; Rothlisberger, D. A strategy for preclinical formulation development using GastroPlus as pharmacokinetic simulation tool and a statistical screening design applied to a dog study. *Eur. J. Pharm. Sci.* **2006**, *27* (1), 91−99.
(41) Fernandez-Teruel, C.; Gonzalez-Alvarez, I.; Navarro-Fontestad, C.; Garcia-Arieta, A.; Bermejo, M.; Casabo, V. G. Computer simulations of bioequivalence trials: selection of design and analyte in BCS drugs with first-pass hepatic metabolism: Part II. Non-linear kinetics. *Eur. J. Pharm. Sci.* **2009**, *36* (1), 147−156.
(42) Parrott, N.; Lave, T. Prediction of intestinal absorption: comparative assessment of GASTROPLUS and IDEA. *Eur. J. Pharm. Sci.* **2002**, *17* (1−2), 51−61.
(43) Willmann, S.; Lippert, J.; Schmitt, W. From physicochemistry to absorption and distribution: predictive mechanistic modelling and computational tools. *Expert Opin. Drug Metab. Toxicol.* **2005**, *1* (1), 159−168.
(44) Jadhav, G. S.; Vavia, P. R. Physicochemical, in silico and in vivo evaluation of a danazol-beta-cyclodextrin complex. *Int. J. Pharm.* **2008**, *352* (1−2), 5−16.
(45) Darwich, A. S.; Neuhoff, S.; Jamei, M.; Rostami-Hodjegan, A. Interplay of metabolism and transport in determining oral drug absorption and gut wall metabolism: a simulation assessment using the "Advanced Dissolution, Absorption, Metabolism (ADAM)" model. *Curr. Drug Metab.* **2010**, *11* (9), 716−729.
(46) Tam, D.; Sun, H.; Pang, K. S. Influence of P-glycoprotein, transfer clearances, and drug binding on intestinal metabolism in Caco-2 cell monolayers or membrane preparations: a theoretical analysis. *Drug Metab. Dispos.* **2003**, *31* (10), 1214−1226.
(47) Yu, L. X.; Lipka, E.; Crison, J. R.; Amidon, G. L. Transport approaches to the biopharmaceutical design of oral drug delivery systems: prediction of intestinal absorption. *Adv. Drug Delivery Rev.* **1996**, *19* (3), 359−376.
(48) Agoram, B.; Woltosz, W. S.; Bolger, M. B. Predicting the impact of physiological and biochemical processes on oral drug bioavailability. *Adv. Drug Delivery Rev.* **2001**, *50* (Suppl. 1), S41−S67.
(49) Zhang, X.; Lionberger, R. A.; Davit, B. M.; Yu, L. X. Utility of physiologically based absorption modeling in implementing Quality by Design in drug development. *AAPS J.* **2011**, *13* (1), 59−71.
(50) Kaddoumi, A.; Fleisher, D.; Heimbach, T.; Li, L. Y.; Cole, S. Factors influencing regional differences in intestinal absorption of UK-343,664 in rat: possible role in dose-dependent pharmacokinetics. *J. Pharm. Sci.* **2006**, *95* (2), 435−445.
(51) Walker, D. K.; Beaumont, K. C.; Comby, P.; Evans, K. M.; Gedge, J. I.; Halliday, R. C.; Roffey, S. J.; Wright, P. A. Pharmacokinetics and metabolism of a selective PDE5 inhibitor (UK-343,664) in rat and dog. *Xenobiotica* **2001**, *31* (8−9), 651−664.
(52) Abuasal, B.; Sylvester, P. W.; Kaddoumi, A. Intestinal absorption of gamma-tocotrienol is mediated by Niemann-Pick C1-like 1: in situ rat intestinal perfusion studies. *Drug Metab. Dispos.* **2010**, *38* (6), 939−945.
(53) Volgyi, G.; Baka, E.; Box, K. J.; Comer, J. E.; Takacs-Novak, K. Study of pH-dependent solubility of organic bases. Revisit of Henderson-Hasselbalch relationship. *Anal. Chim. Acta* **2010**, *673* (1), 40−46.
(54) Avdeef, A.; Bendels, S.; Di, L.; Faller, B.; Kansy, M.; Sugano, K.; Yamauchi, Y. PAMPA—critical factors for better predictions of absorption. *J. Pharm. Sci.* **2007**, *96* (11), 2893−2909.
(55) Zakeri-Milani, P.; Valizadeh, H.; Tajerzadeh, H.; Azarmi, Y.; Islambolchilar, Z.; Barzegar, S.; Barzegar-Jalali, M. Predicting human intestinal permeability using single-pass intestinal perfusion in rat. *J. Pharm. Pharm. Sci.* **2007**, *10* (3), 368−379.
(56) Kim, J. S.; Mitchell, S.; Kijek, P.; Tsume, Y.; Hilfinger, J.; Amidon, G. L. The suitability of an in situ perfusion model for permeability determinations: utility for BCS class I biowaiver requests. *Mol. Pharmaceutics* **2006**, *3* (6), 686−694.
(57) Obach, R. S.; Baxter, J. G.; Liston, T. E.; Silber, B. M.; Jones, B. C.; MacIntyre, F.; Rance, D. J.; Wastall, P. The prediction of human pharmacokinetic parameters from preclinical and in vitro metabolism data. *J. Pharmacol. Exp. Ther.* **1997**, *283* (1), 46−58.
(58) Poulin, P.; Theil, F. P. Prediction of pharmacokinetics prior to in vivo studies. 1. Mechanism-based prediction of volume of distribution. *J. Pharm. Sci.* **2002**, *91* (1), 129−156.
(59) Rodgers, T.; Rowland, M. Mechanistic approaches to volume of distribution predictions: understanding the processes. *Pharm. Res.* **2007**, *24* (5), 918−933.
(60) Lave, T.; Coassolo, P.; Reigner, B. Prediction of hepatic metabolic clearance based on interspecies allometric scaling techniques and in vitro-in vivo correlations. *Clin. Pharmacokinet.* **1999**, *36* (3), 211−231.
(61) Mouly, S.; Paine, M. F. P-glycoprotein increases from proximal to distal regions of human small intestine. *Pharm. Res.* **2003**, *20* (10), 1595−1599.
(62) Bruyere, A.; Decleves, X.; Bouzom, F.; Ball, K.; Marques, C.; Treton, X.; Pocard, M.; Valleur, P.; Bouhnik, Y.; Panis, Y.; Scherrmann, J. M.; Mouly, S. Effect of Variations in the Amounts of P-Glycoprotein (ABCB1), BCRP (ABCG2) and CYP3A4 along the Human Small Intestine on PBPK Models for Predicting Intestinal First Pass. *Mol. Pharmaceutics* **2010**, *7* (5), 1596−1607.
(63) Zhang, Y.; Benet, L. Z. Characterization of P-glycoprotein mediated transport of K02, a novel vinylsulfone peptidomimetic cysteine protease inhibitor, across MDR1-MDCK and Caco-2 cell monolayers. *Pharm. Res.* **1998**, *15* (10), 1520−1524.
(64) Korjamo, T.; Kemilainen, H.; Heikkinen, A. T.; Monkkonen, J. Decrease in intracellular concentration causes the shift in Km value of efflux pump substrates. *Drug Metab. Dispos.* **2007**, *35* (9), 1574−1579.